Heritage Science

RESEARCH

Open Access

Modelling of hygro-mechanical behaviour of wooden panel paintings: model calibration and artworks characterisation

Lorenzo Riparbelli[1], Paola Mazzanti[1*], Thomas Helfer[2], Chiara Manfriani[1], Luca Uzielli[1], Ciro Castelli[3], Andrea Santacesaria[3], Luciano Ricciardi[3], Sandra Rossi[3], Joseph Gril[4,5] and Marco Fioravanti[1]

Abstract

Wooden Panel Paintings (WPP) are among the most significant historical and artistic artifacts from the Middle Ages and Renaissance and pose a challenge to conservators and scientists in both their comprehension and conservation. From a structural point of view, they can be considered as multi-layered objects, consisting of a wooden support and several pictorial layers. The wooden support, hygroscopic in nature, constantly seeks equilibrium with the humidity of the environment, and consequently deforms. Based on a series of hygroscopic tests carried out on six original WPPs, the present work aims to model their deformation tendencies induced by moisture changes and to characterise them by means of an inverse identification process. The sensitivity analysis of this study provided valuable insights into the complexity of the phenomenon of WPP deformation: even small variations in input variables (board anatomy, stiffness and emissivity of pictorial layers) led to significant changes in the deformation trend over time, highlighting the high variability of the physical problem under investigation. Sobol's analysis variance confirmed this complexity, demonstrating the different levels of influence of input variables and the existence of interactions between them. Overall, the results of this analysis highlighted the need to carefully evaluate the interactions and uncertainties in input variables to fully understand the complexity of the system. The iterative optimization process led to numerical results tending to agree with experimental data, with most results showing a very high correlation. This suggests that the chosen variables and modelling assumptions sufficiently described the physical system and that numerical models can be accurately calibrated. The proposed concept of 'learning from objects', by conducting experimental investigations specifically dedicated to understanding the deformation tendencies of the artwork, is essential. In this approach, numerical analysis is used in conjunction with experiments to gain a deeper understanding of the artwork, characterise it and extract valuable information.

Keywords Wooden panel paintings, Conservation, Experimental tests, Numerical modelling, Panel painting deformation tendencies, Paint layer emissivity, Paint layer stiffness

*Correspondence:
Paola Mazzanti
paola.mazzanti@unifi.it
[1] DAGRI, University of Florence, Florence, Italy
[2] CEA, DES, IRESNE, DEC, Cadarache, 13108 Saint-Paul-Lez-Durance, France
[3] Opificio Delle Pietre Dure, Florence, Italy
[4] Université Clermont Auvergne, INRAE, PIAF, Clermont-Ferrand, France
[5] Université Clermont Auvergne, CNRS, Institut Pascal, Clermont-Ferrand, France

Introduction

Wooden Panel Paintings (WPPs) represent one of the most important categories of cultural artefacts, whose conservation is challenging due to their interaction with environments. Although the early treatises [1] attempt to codify both structure and construction techniques, WPPs, while maintaining common denominators over time, may differ from case to case according to different schools and workshops [2, 3], resulting in a wide

panorama of morphological, constructional and manufacturing diversities, which is combined with the intrinsic variability of wood. This structure, together with its interaction with the environment, can lead to the appearance of mechanical stresses that can be critical for the conservation of a WPP, being at the origin of permanent deformations, cracks, or damages to paint layers. Each artwork shows its own deformation behaviour that may be explained through generative causes such as:

1. Wood hygroscopicity: wood being a hygroscopic and anisotropic material, environmental hygrothermal fluctuations can produce permanent deformations, induced by the combined effect of wood anisotropy with respect to the board cut, transient deformation induced internal humidity gradients, and the compression set phenomenon (i.e. the permanent deformation deriving from the succession of environmental fluctuations over time [4]).
2. Mechanical asymmetry: stiffness asymmetry within the thickness may be due to differences between the wood and paint layers, to the wood itself as it presents a non-homogeneous stiffness following growth rings and main anatomical directions, and to the interaction with any restraining system such as frames and crossbeams. Moreover, the shrinking-swelling behaviour of wood is orders of magnitude bigger than that of the paint layers [5].
3. Ageing: over time biological, physical, and chemical agents may cause permanent modification (ageing phenomena) that can affect the behaviour of wood, paint layers, glues and of their mutual interactions.
4. Anthropic: past human interventions such as restoration, size adjustments, accidents and tampering, exposure to sudden winter heating, etc.

Each of these aspects has been the object of several specific research works. Studies and monitoring of original works have been carried out in the past [6–8] including using optical measurement methods to correlate deformation fields with the mechanical characteristics of the paint layers [9]. Materials used to make the WPPs were object of characterisation by [5, 10, 11] for the wooden support, as well as [12] for the stiffness and [13–15] for the emissivity characteristics of the painted layers. Most parts of this latter studies were carried out on new materials, because sampling on original components of WPPs is impossible, producing a limited representativity of the behaviour of real materials subjected to centuries of ageing and interacting each other inside the structure, as a recent research shows [16]. Such paper shows that the main parameters responsible of the hygro-mechanical behaviour of the WPPs are the tree ring orientation of the wooden panels, the stiffness of the ground layers and the emissivity of the varnishes (and their interactions). Within the same research, a classificatory model was developed which shows that the hygro-mechanical behaviour of the WPPs is complex and hardly predictable if the characteristics of the material making the WPP are considered independent. It is their interaction, indeed, which strongly affects the hygro-mechanical behaviour of the WPP.

Models of the dynamics of panel paintings have been also developed [17, 18], sometime considering a painting with a complex structure subject to environmental variations [19]. To these studies shall also be added those on wood-moisture interaction [20], on cracking phenomena of paint layers [21], on the response of painted panels to humidity variation [22], and finally one on the analysis of the effect of relative humidity cycles [23]. Some studies were also carried out on replicas and simulacra [21, 24–26].

Numerical studies mainly use literature values to define hygro-mechanical characteristics, opening up the risk of reaching unrealistic solutions [27]. In fact, key variables such as anatomical directions, stiffness and emissivity of the paint layers can generate a wide field of deformation patterns both qualitatively and quantitatively, as it has been demonstrated by numerical modelling and monitoring of original artworks [16]. This approach is certainly the most applied in literature, where non-original materials and mock-ups are tested separately and their values are then used to construct models. It operates with a logic where the behaviour of a WPP results from the additive contribution of each individual non-original component of the system.

The present work takes a different methodological perspective, considering the WPP as a complex system, where initial conditions, time history and evolution are unknown. This implies that small variations of individual variables, and even more so the variations of these variables in relation to the values of others [16], cannot be predicted through studies conducted on artificial samples, copies, materials that have not been aged or subjected to artificial ageing cycles. The resulting top-down approach starts from the awareness that the behaviour of complex systems can often only be measured and needs to be addressed through tests performed on historical objects, without aprioristic considerations on aspect that cannot be directly measured and observed. It is based on known hygro-mechanical models and aims to calibrate their characteristics through non-destructive experimental tests conducted on individual artworks. This approach consists in not worrying aprioristically about the structural composition, but representing all the physical entities with characteristics that, in their interaction, provide

us with a model that behaves similarly to an original when subjected to experimental characterisation tests. In this interpretation, after an established theoretical approach and sound physical–mathematical methods have been set up, the numerical analyses become a way of extracting advanced information from experimental evidence that does not provides it directly.

The aim of the present study is to broaden the current spectrum of knowledge of the main deformation drivers of real WPPs from an experiment on six original paintings subjected to micro changes in humidity, and to draw analytical conclusions.

The research builds on a previous work [16] that was carried out by means of experimental tests on 6 original WPPs subjected to slight variations in humidity inside a climatic chamber and the measurement of the resulting deflection. The cycles were repeated after applying an aluminium foil to waterproof the painted face of the panel paintings, in a way that does not affect the rigidity of the painted layers. This allowed the stiffness and emissivity characteristics of the original paintings to be qualitatively determined by non-invasive experimental tests.

In continuation of this work, the present research proposes to determine, in a non-invasive manner, the hygro-mechanical characteristics of the six original WPPs studied and to calibrate their respective numerical models. The work presents a reproducible method, based on a finite element calculation, for the direct characterisation of a WPP by means of an experimental test in which the work is subjected to a slight change in humidity [16].

Materials and methods

The panel paintings and experimental set up

The study was carried out on six original WPPs of the Italian painting school. Each one is made of poplar wood (*Populus* sp) and was selected based on its representativeness in terms of construction period, structural typology, thickness of the preparatory layers, presence or absence of canvas. Their main technical specifications are given in Table 1 and in [16].

Each panel was equipped with a Deformometric Kit (DK), as described in "The measure of the cupping angle" section, and subjected to controlled variations of relative humidity (RH) to measure its hygroscopic deformation. The restraint system was removed to allow only hygroscopic deformation without influence of the crossbeams. A special climatic box was built in the Opificio delle Pietre Dure restoration laboratories; the RH was controlled by means of a humidifier (Preservatech miniOne) and ventilation was provided by means of 6 fans and the usual operation of the humidifier itself. RH and temperature (T) were monitored in real time using URT Smart CEAM LoRa-C (±2% e ±0.5 °C), 1 point every 15 min. The data were continuously collected by means of CEAM CWS software, an integrated platform for monitoring, control and shared management based on web-cloud-IoT technology. The panel paintings were arranged in the climatic box in a vertical position, and the contact area was covered with PTFE to eliminate friction. Inside the box, the RH values varied between 50 and 65%. Seven humidity step changes were performed: 3 desorption and 4 adsorption tests. The hygroscopic tests were carried out under two different boundary conditions: (a) the front face free to exchange moisture with the environment (2 in desorption and 3 in adsorption) and (b) the front face sealed by an aluminium foil (1 in desorption and 1 in adsorption). This method makes it possible to measure the actual emissivity of the front surface, i.e. the paint layers and varnish, and its effect on the deformation behaviour of the artworks. Details are given in [16]. The surface emissivity does not depend solely on the material itself, but rather characterises the resistance present in the surface transport process. This resistance can be due to factors such as a thin coating or the Brownian motion of the air, which can lead to changes in the relative humidity (RH) at the surface (air speed can significantly affect the effect of the latter factor). Generalising the surface

Table 1 Description of the six paintings: dimensions, materials and characteristics

	WPP1	WPP2	WPP3	WPP4	WPP5	WPP6
Dimensions	530×900x14 mm	67×1310x33 mm	700×1370x25 mm	645×775x23 mm	655×855x30 mm	650×890x28 mm
Wood species	*Populus alba* L	*Populus alba* L	*Populus alba* L	*Populus alba* L	*Populus alba* L	*Populus alba* L
Boards	2 T boards (~40 mm from pith), 275 and 255 mm wide	3 R boards 170, 380 and 145 mm wide	4 boards; 1 T (~50 mm from pith) 185 mm wide; 3 R 165, 130 and 220 mm wide	2 T boards (~20 mm from pith), 210 and 435 mm wide	2 T boards (~50 mm from pith), 210 and 435 mm wide	3 boards; 1R 225 mm wide; 2 T (~60 mm from pith), 320 and 105 mm wide
Ground layer	Thick	Thick	Thick	Thick	Thin	Thin

R board: quartersawn board, cut along a radius of the stem; T board: flatsawn board, cut orthogonally to a radius of the stem, at a certain distance from the pith estimated on a face [16]

emission factor from panel to panel or under different environmental conditions (air turbulence) will result in uncertainty.

The measure of the cupping angle

The Deformometric Kit (DK, [28]) is a measuring device conceived for monitoring the deformation dynamics of wooden objects, mainly in relation to fluctuations of the surrounding environmental conditions (Fig. 1); it has been used in many study campaigns, mainly on WPPs [7, 29–32].

Since the objective of this study is the calibration of a model, we considered parameters that were not subject to any assumptions, but only to direct measurement: the deformation, or equivalently the change in length, of the measurement lines, and the derived cupping angle. These measurements are agnostic to both the physical phenomenon that generated the variation in relative inclination between the two sections and the characteristics of the material that lies between the two columns. Therefore, the deformations of both measurement lines were chosen as parameters for calibrating the numerical models.

Furthermore, this parameter has a clear, well-known and understandable physical meaning in the field of WPP conservation.

Optimisation procedures (described below in "Computation of the equilibrium moisture content" section) require that the correct experimental value can be determined at any given time, so the raw data were treated according to [33]. An interpolation procedure was applied to all data, locally fitted to a second order polynomial curve using a Gaussian kernel to weight the data. The standard deviation used for the kernel (50000 s) represents the window in which the polynomial interpolation is performed.

Numerical modelling

For the objectives of this study, the role of the numerical model is to serve as a means of interpreting and enhancing comprehension of the experimental findings, and to reveal the interdependent relationships among the variables that influence the behaviour of the underlying physical model. In this respect, numerical modelling has been used to evaluate, through an optimization algorithm, the influence and the mutual interactions of the identified dimensioning variables (layers stiffness, moisture diffusion and emissivity, anatomical cut) in determining the deformation tendency of the painted board.

For general modelling principles we refer to [16], listing below only those elements in which this modelling differs.

We applied the following boundary condition to model the global emissivity of the rear, bare wood, face:

$$\frac{q_t}{\rho_0} = E_{c1} \cdot (m_{r,air} - m_{r,sur}) \tag{1}$$

where $m_{r,air}$ is the wood equilibrium moisture content corresponding to the air humidity, $m_{r,sur}$ is the moisture

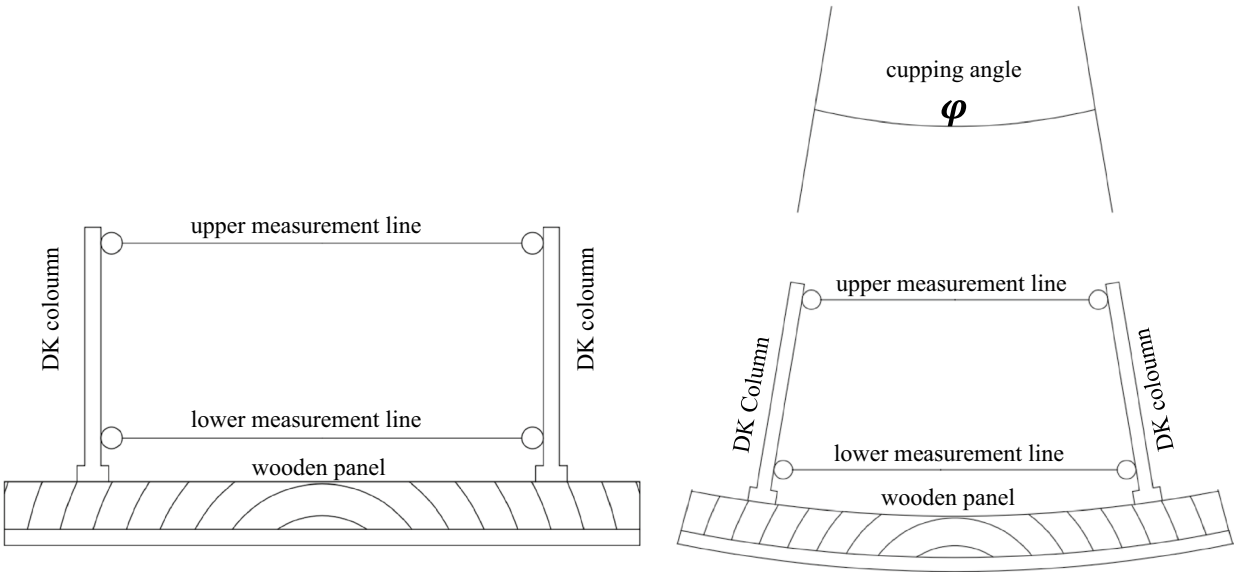

Fig. 1 On the right the general set up of DK on a wood board of a WPP, on the right the physical meaning of the cupping angle and its measurement with the DK

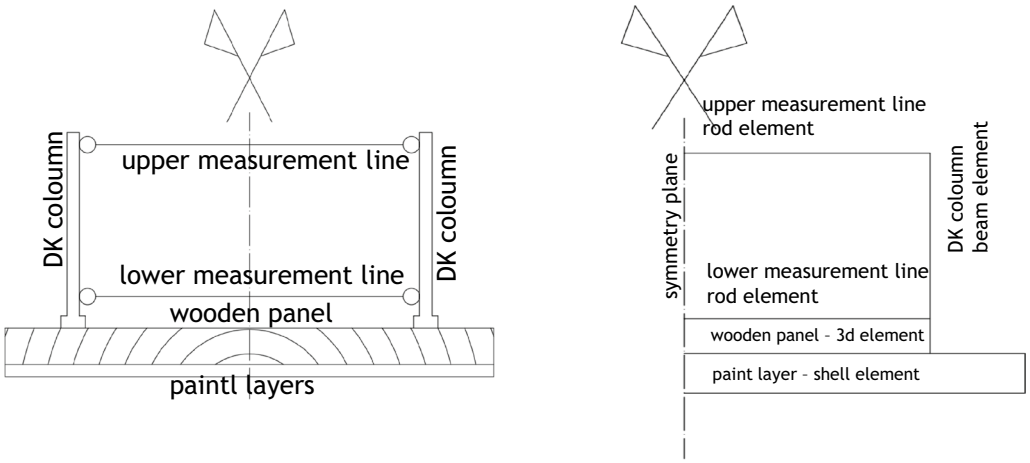

Fig. 2 Scheme of the modelling: on the left the real case, on the right the optimization simplified case with the optimization choices in terms of finite elements

content of the rear wood surface calculated by the solver, and $\mathbf{E_{c1}}$ is the global effective emissivity of the back of the painting, taking into account also possible aging effects and protective treatments that may affect the emissivity of this surface.

The geometry and discretisation were carried out with the open-source software Salome-Meca developed by EDF (Électricité de France), the simulations with the open-source solver code_aster [34], and the handling of cylindrical coordinates in the solution of the computational model, both for elasticity and swelling, with the open-source software Mfront [35], see Annex 1.

As both the optimization process and the sensitivity study are computationally intensive, it was essential to reduce the degrees of freedom of the system as much as possible. The following assumptions were made in the modelling:

- The length parallel to the grain of the wood panels was reduced to 400 mm (a preliminary feasibility study showed that mechanical edge effects lose their influence at a distance of about 150 mm from the longitudinal ends in a WPP without crossbeam).
- In the transversal direction, considering that the DKs were mounted in the exact centre of symmetrical panels, only half a panel was modelled with symmetry constraints and isostatic condition (Fig. 2).
- The edge effect between adjacent boards is considered negligible considering that they are glued at the edge, the preservation of plane sections, the absence of stiffeners or cross beams and the freedom to deform given the external isostatic constraints (verified in the preliminary feasibility study).
- The thickness of the panel was sliced into 30 layers to capture small local variations due to the internal moisture gradient.
- The panel equipped with the DK is not subjected to external forces; it deforms only as a result of internal hygroscopic interactions.

The output parameters are the deformations of the two measurement lines and, derived from them, the cupping angle, defined as the angular rotation of the section below the DK column. This ensures the biunivocality of the boundary conditions between the numerical model and the experimental data. A similar method for comparing experimental results and numerical models is described in [16].

Computation of the equilibrium moisture content

The calculation of the equilibrium moisture content (EMC) is required to attribute the correct hygro-mechanical boundary conditions for the moisture. It was made following [36] that permits to calculate and describe the sorption isotherms in wood, with changing temperature and partial cycles. The model is based on [36], that relates relative humidity (*RH*) to EMC value, noted *w*, as follows:

$$w = w_{ad}(RH, T) = w_s(T).[\varphi_{ad}.\ln(RH).\exp(\alpha_{ad}.RH)] \quad \text{for adsorption} \tag{2}$$

$$w = w_{de}(RH, T) = w_s(T).[\varphi_{de}.\ln(RH).\exp(\alpha_{de}.RH)] \quad \text{for desorption} \tag{3}$$

with w_s the EMC value at 100%RH; $w_{ad}(RH, T)$ and $w_{de}(RH, T)$ the adsorption and desorption curve, respectively, for a given temperature T;α_{ad},α_{de}, φ_{ad}, φ_{de} constant values. The effect of the temperature, following [37] and based on the work of [38], is concentrated on FSP leading to a general form of $w_s(T)$:

$$w_s(T) = \left(w_s^0 + \frac{C_{anh}}{C_w}\right) \cdot \exp\left(-\frac{C_w}{L} \cdot T\right) - \frac{C_{anh}}{C_w} \tag{4}$$

with w_s^0 the FSP at 0 °C, C_{anh} the heat capacity of the oven dry material, C_w the heat capacity for the bound water, L the latent heat of state change.

For the calculation of the EMC evolution from a given condition given by w_0 and RH_0 (Fig. 3), the situations of adsorption and desorption are distinguished:

$$\left(\frac{\mathrm{d}w}{\mathrm{d}RH}\right)_{ads} = \frac{A.(w_0 - w_{ad})^C.w'_{de}(w_0) + (w_{de} - w_0)^C \cdot w'_{ad}(w_0)}{(w_{de} - w_{ad})^C}$$
$$\text{with}\left(\frac{\mathrm{d}w}{\mathrm{d}RH}\right)_{ads} > 0 \text{ (adsorption)} \tag{5}$$

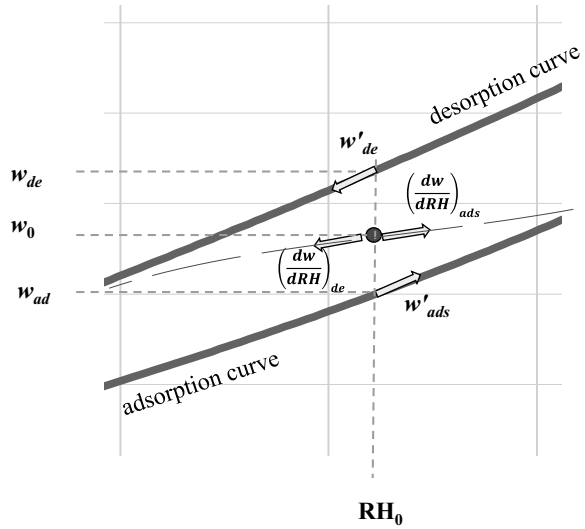

Fig. 3 Partial isotherm behaviour. The parameters are from Eqs. (9) and (10)

$$\left(\frac{\mathrm{d}w}{\mathrm{d}RH}\right)_{des} = \frac{(w_0 - w_{ad})^C \cdot w'_{de}(w_0) + B \cdot (w_{de} - w_0)^C \cdot w'_{ad}(w_0)}{(w_{de} - w_{ad})^C}$$
$$\text{with}\left(\frac{\mathrm{d}w}{\mathrm{d}RH}\right)_{des} < 0 \text{ (desorption)} \tag{6}$$

where the constants A and B define the slope ratio for a path toward the absorption or the desorption isotherm, respectively, and C is a calibration coefficient.

The material coefficient chosen for the current study, given in Table 2, are those proposed by [36].

The time-history of RH and T variation described in [16] was modelled on the basis of the above theory, using a simplified step-wise approximation of RH history and constant T, as shown in Fig. 4. The results in terms of MC for each experimental step is given in Table 3. The values then chosen as boundary conditions for the steps used in the optimization process are listed in Table 4.

Table 3 Relative humidity steps, Temperature, and, based on that, calculated EMC variation for all tests

Test name	ΔRH step [%]	T [°C]	ΔEMC step calculated [%]
DES 1 Not waterproofed	62–52	23	−0.98
ADS 1 Not waterproofed	52–61	23	0.74
DES 2 Not waterproofed	61–56	23	−0.43
DES 3 Not waterproofed	56–51	23	−0.44
ADS 2 Not waterproofed	51–60	23	0.62
DES 4 Waterproofed	60–53	23	−0.63
ADS 3 Waterproofed	53–60	23	0.59

Table 2 Values for the moisture content evaluation

A	B	C	w_0	φ_{ad}	α_{ad}	φ_{de}	α_{de}
0.4	0.06	1.5	0.3236	0.8490	1.647	0.8520	1.088

Fig. 4 Time History of Temperature (T) and relative humidity (RH) over the whole experimental campaign: in blue the measured RH, in black the simplified RH used for the EMC calculation

The previous RH history being unknown, in the initial state the value of w was assumed to be mid-way between absorption and desorption isotherms.

Table 4 Values of the EMC steps used for modelling

WPP	Delta EMC waterproofed [%]	Delta EMC not waterproofed [%]
1	0.59	0.74
2	−0.63	−0.44
3	−0.63	−0.44
4	−0.63	−0.44
5	−0.63	−0.98
6	−0.63	−0.44

Optimization

An iterative optimization algorithm was chosen to calibrate the numerical model to fit the experimental data, allowing to calculate the hygro-mechanical parameters for each of the six planks. The cost functional *J,* object of the minimization, is given as a function c, vector of the n parameters to be identified:

$$J(c) = \|\varepsilon - \varepsilon_{exp}\| \tag{7}$$

where ε are the values of time-history of deformation of the DK measurements lines calculated via numerical methods, ε_{exp} are the corresponding experimentally determined values and $\|\cdot\|$ is a norm on L, space of the observable values. Minimisation was performed by means of a technical solution [39] based on the succession of a genetic algorithm followed by a Nelder Mead-type minimisation scheme. This proves to be a very effective method [40, 41] for finding solutions when, in general, a small variation in the coefficients objects of the minimization generates considerable variations in the results.

The parameters subjected to the identification process are as follows:

1. The coefficient of diffusion D_0
2. The emissivity of the back E_{c1}
3. The Young modulus of the paint layer E_p
4. A coefficient X that multiplies the tensor of hygromechanical deformation $\underline{\underline{\varepsilon_{hyg}}}$:

$$\underline{\underline{\varepsilon_{hyg}}} = X \cdot \underline{\underline{\alpha}} \cdot \Delta w \tag{8}$$

Where $\underline{\underline{\alpha}}$ is the tensor of hygroexpansion rate and Δw is the variation of moisture content. The significance, therefore, of this coefficient is to globally calibrate the hygroscopic strain variation associated with a change in moisture content; for this reason, it is simultaneously a multiplier of both the shrinkage/swelling coefficient and the Delta w value obtained from the Varnier-Merekeb-Pedersen theory used here. In fact, on the one hand the aforementioned theory uses a variety of coefficients that cannot be calibrated to the individual painting, mainly due to the fact that they require dangerous humidity variations or destructive investigations, on the other hand it is not possible to precisely establish the climatic history of the paintings prior to the start of the tests and therefore

Table 5 Mechanical and physical initial properties

Wood young moduli	$E_L = 10{,}060$ MPa	$E_R = 641$ MPa	$E_T = 306$ MPa
Wood shear moduli	$G_{RT} = 200$ MPa	$G_{TL} = 640$ MPa	$G_{LR} = 860$ MPa
Wood Poisson's ratios	$\nu_{RT} = 0.7$	$\nu_{LT} = 0.47$	$\nu_{LR} = 0.46$
Wood shrinkage	$\alpha_L = 0.39\%/\%$	$\alpha_R = 1.92\%/\%$	$\alpha_T = 3.45\%/\%$
Coefficient of moisture diffusion in wood	$D_{0=} 1.52 \cdot 10^{-4}$ mm^{2}s^{-1}		
Front emissivity	$E_c = 1.0 \cdot 10^{-5}$ mm·s^{-1}		
Back emissivity	$E_{c1} = 1.0 \cdot 10^{-5}$ mm·s^{-1}		
Paint layers young modulus	$E_p = 1000$ MPa		
Paint layers Poisson 's ratio	ν_p =0.2—not subjected to optimization		
X	1		
Y	1		

the starting point within the hygroscopic hysteresis is arbitrary and chosen by us as equidistant between the limit isotherms of absorption and desorption. It should also be pointed out here that it is not possible to dissociate the two components in a heuristic characterisation process because the two components have the same effect on the overall deformation behaviour, making their dissociation impossible. For all these reasons we decided to calculate, via optimization, two different X value (X wp, Waterproofed—X no wp, not Waterproofed) for the two kind of tests done.

5. A Y coefficient that multiplies/divides the fourth-order compliance tensor in the following way:

$$Y^{-1} \cdot \underline{\underline{S_{ij}^0}} = \begin{pmatrix} Y^{-1}S_{11}^0 & Y^{-1}S_{12}^0 & Y^{-1}S_{13}^0 & 0 & 0 & 0 \\ Y^{-1}S_{12}^0 & Y^{-1}S_{22}^0 & Y^{-1}S_{23}^0 & 0 & 0 & 0 \\ Y^{-1}S_{13}^0 & Y^{-1}S_{23}^0 & Y^{-1}S_{33}^0 & 0 & 0 & 0 \\ 0 & 0 & 0 & Y^{-1}S_{44}^0 & 0 & 0 \\ 0 & 0 & 0 & 0 & Y^{-1}S_{55}^0 & 0 \\ 0 & 0 & 0 & 0 & 0 & Y^{-1}S_{66}^0 \end{pmatrix} \quad (9)$$

6. The emissivity of the paint layers E_c

The rigidity components, the initial shrinking/swelling coefficients and the initial diffusion used for poplar wood reported in Table 5 are based on [10] and [18].

A first optimisation process is carried out on parameters 1–6 on the cupping angle time history of the painting with the waterproofed front; in fact, in this case, the flow of moisture transiting the painting surface is identically null and the calculation of the emissivity of the painting front is meaningless.

A second process is subsequently performed on parameters 4 and 6, on the painting with the non-waterproofed front, leaving parameters 1,2,3,5 identified in the previous optimisation process unchanged.

This process also provides us with a cross-validation in the second analysis of the results obtained in the first one; in fact, the fitting of the second one takes place for internal moisture distributions that are completely different from the first one, varying only two variables, emissivity of the front and coefficient of hygroexpansion. Therefore, its conformity with the experimental data confirms the goodness of the first analysis carried out, whose results in terms of (wood diffusion, back emissivity, wood stiffness, paint layer stiffness) remained identical in the second.

Sensitivity analysis

In order to be able to use an inverse identification system, it is necessary to carry out a sensitivity study on the parameters under study.

Sensitivity analyses allow us to understand which inputs to a model contribute most to the variability of the output, and more specifically to understand input–output relationships, determine the magnitude of the contribution of input uncertainties on the model's output, identify the significance and magnitude of the inputs on the output, and guide modelling and experimental choices.

The opensource software Persalys [42], which is based on the highly industry-validated openTurns methods [43] was used to handle uncertainties and variability. This software can be easily coupled with code_aster, allowing investigations, in our case of sensitivity, to be performed on a finite element model in a fast and rigorous manner.

A Sobol sensitivity analysis is a type of statistical analysis that helps to identify which variables in a model have the most significant impact on its output. In the context of a finite element model, this means that Sobol's method is used to determine which input variables (such as material properties or boundary conditions) are most responsible for affecting the behaviour of the model.

One of the main advantages of using Sobol's method is that it is able to handle non-additive, non-monotonic, and non-linear systems. In other words, it can accurately assess the influence of input variables even when the

relationships between those variables and the model output are complex and nonlinear.

However, Sobol's method is computationally intensive, meaning that it can be time-consuming and resource-intensive to implement. Despite this, it is still a valuable tool for exploring all areas of the input space, as it allows for the consideration of interactions and nonlinear responses. This means that it can help to identify unexpected relationships between variables and their impact on the model output, which might not be apparent through other methods of sensitivity analysis. Overall, the use of Sobol's method in a sensitivity analysis on a finite element model can provide important insights into the behaviour of the model and the variables that most strongly influence its output. Following the work of [44] and [45], in our sensitivity analysis we want to represent the studied model as:

$$Y = \mathcal{H}(X_1, \ldots, X_n) \tag{10}$$

where the scalar Y denotes the variable of interest, here the cupping angle; $\mathcal{H}$ is the model, deterministic or stochastic, that governs the problem, here the finite elements model; and $X_1, \ldots, X_n$ are the input variables.

The variance of Y can be decomposed as:

$$V(Y) = \sum_i V_i + \sum_i \sum_{j>i} V_{ij} + \ldots + V_{123\ldots n} \tag{11}$$

with $V_i = V(E(Y|X_i))$ the first-order partial variance, $V_{ij} = V(E(Y|X_i, X_j)) - V_i - V_j$ the second-order partial variance, and so on. V_i quantifies the influence of X_i on the dispersion of Y, while V_{ij} measures the second-order interaction contribution between X_i and $X_j to V(Y)$.

Normalizing the partial variances $V_i, V_{ij}, \ldots V_{123\ldots n}$ with the total variance we obtain the Sobol sensitivity indices, here for first and second orders:

$$S_i = \frac{V_i}{V(Y)}, S_{ij} = \frac{V_{ij}}{V(Y)} \tag{12}$$

We may derive also a Sobol total index [46] for the input i variable, as:

$$ST_i = 1 - \frac{V(E(Y|X_{-i}))}{V(Y)} \tag{13}$$

where X_{-i} is the vector of all parameters except i.

For a general X_i the difference between the total index and the first-order index is the amount of interaction that X_i contributes to.

In a Sobol sensitivity analysis, the first-order index and total index are two commonly used measures of the sensitivity of a model output to its input parameters.

The first-order index measures the fractional contribution of an individual input parameter to the overall variance of the model output. It quantifies the extent to which changes in the value of that input parameter alone affect the variability of the output, without considering any interaction effects with other input parameters. Specifically, it is defined as the ratio of the variance of the model output due to the variation of the individual input parameter, to the total variance of the model output. The first-order index is a measure of the individual importance of a single input parameter, and can be used to rank the input parameters in terms of their relative importance.

The total index, on the other hand, takes into account the effects of interactions between input parameters of different orders. It evaluates the full range of parameter space by considering all possible combinations of input parameters and their interactions. Specifically, it measures the total contribution of each input parameter, including its first-order effects and all higher-order interactions, to the overall variance of the model output. The total index provides a more comprehensive measure of the impact of an input parameter on the model output, by considering not only its individual effect but also its combined effect with other input parameters.

In summary, the first-order index measures the sensitivity of the model output to a single input parameter, while the total index measures the sensitivity of the model output to all input parameters, including their interactions. Both indices are important measures in a Sobol sensitivity analysis as they help identify the most important input parameters in the model and provide insights into the overall behaviour of the model [47].

In a finite element analysis sensitivity study, Sobol's method can be used to identify the impact of input variables (such as material properties, boundary conditions, or geometric parameters) on the output parameters of the model (such as stress, displacement, or strain). Overall, Sobol's method can be a useful tool for improving the accuracy and reliability of finite element analyses by providing insights into the behaviour of the model and its sensitivity to input parameters.

Results

General sensitivity study

Figure 5 reports the result of a sensitivity study of the 'local' type, as in [16, 17], where each variable is varied while the others remain unchanged. This analysis shows the qualitative appropriateness of the choice of parameters, objectified in two main characteristics:

1. Each variation of an individual variable must have a significant impact on the output, in our case the cupping angle.

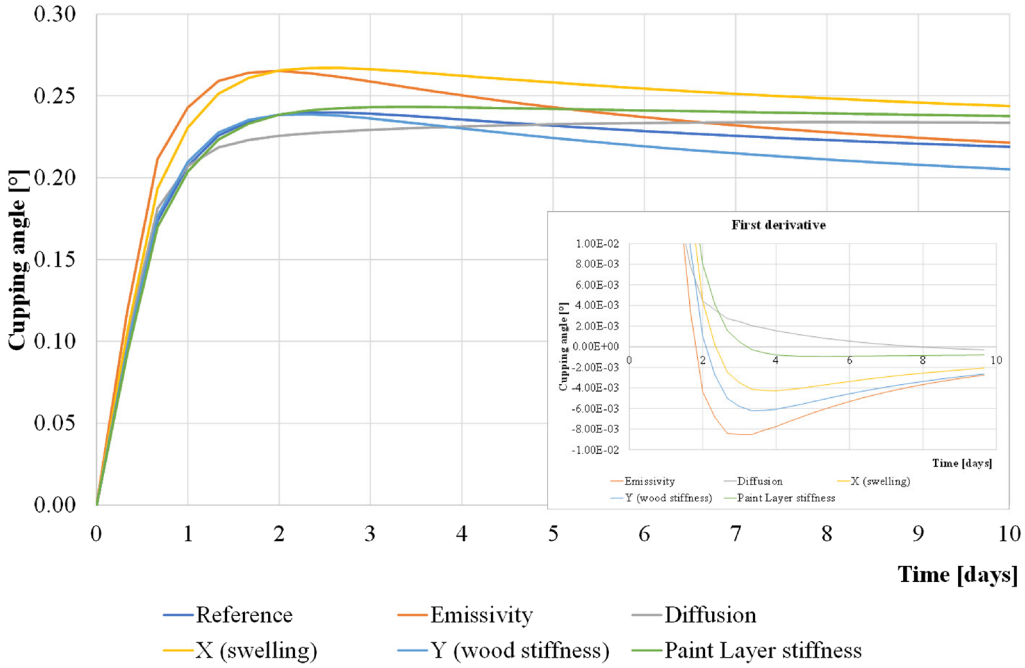

Fig. 5 Results for the sensitivity study according to Table 6. In the window, the first derivative of the curves of the sensitivity study

2. It must give rise to a different curve compared to that generated by the other variables: two variables yielding the same global variation over time would not be distinguishable in an identification process, making it indeterminate.

In order to improve the readability of the graph in Fig. 5 only the results relevant to WPP5 are shown (the others did not show significant differences). They were obtained by applying the variations listed in Table 6 with respect to the values determined in "Hygro-mechanical identification" section. Here, the emissivity of the painted front is excluded from the sensitivity studies, since it was carried out primarily physically, by waterproofing and excluding this variable.

The graph in Fig. 5 clearly shows that all the variables considered have a significant effect on the variation of the cupping angle over time and that each of them can determine curves whose time evolution is significantly different from each other, as clearly shown by the first derivative calculation of these curves (window in Fig. 5). However, the limitation of local sensitivity analysis is that it evaluates one parameter at a time and does not capture the consequences of simultaneous changes in all model parameters, as well as the interactions between parameters.

Sobol sensitivity study

Despite performing a global sensitivity analysis using the Sobol method on five panel paintings, the results were found to be similar in nature. Therefore, only the results related to one specific painting (WPP5) are

Table 6 Values of the hygro-mechanical properties used for the sensitivity study

Model	D_0 [$m^2\ s^{-1}$]	E_p [MPa]	E_c [$m\ s^{-1}$]	E_{c1} [$m\ s^{-1}$]	X waterproofed	Y
Reference	$1.10\ 10^{-09}$	1952	$1.0\ 10^{-10}$	$2.6\ 10^{-07}$	1.27	1.29
Emissivity	$1.10\ 10^{-09}$	1952	$1.0\ 10^{-10}$	**$3.1\ 10^{-07}$**	1.27	1.29
Diffusion	**$2.10\ 10^{-09}$**	1952	$1.0\ 10^{-10}$	$2.6\ 10^{-07}$	1.27	1.29
X	$1.10\ 10^{-09}$	1952	1.010^{-10}	$2.6\ 10^{-07}$	**1.52**	1.29
Y	$1.10\ 10^{-09}$	1952	$1.0\ 10^{-10}$	$2.6\ 10^{-07}$	1.27	**1.39**
Paint stiffness	$1.10\ 10^{-09}$	**2452**	$1.0\ 10^{-10}$	$2.6\ 10^{-07}$	1.27	1.29

In bold the values variated from the reference situation

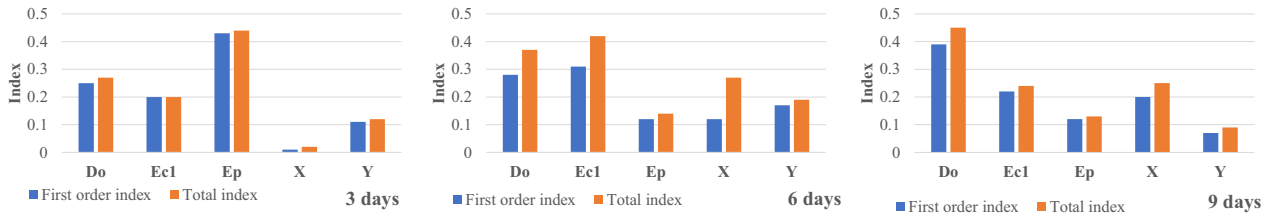

Fig. 6 Sobol's sensitivity analysis for the cupping angle value obtained after 3, 6 and 9 days after the humidity step change (Do -Diffusion coeff., Ec1 Back side emissivity, Ep Rigidity of paint layers, X and Y corrective coeff.s.)

presented here (Fig. 6). The output variable for the analysis was the cupping angle, which was calculated at three different time points (3, 6, and 9 days) after a step change in moisture content (Delta w = −1%) was applied as a boundary condition for the back face, while the front was defined as insulated to moisture flux. To obtain the Sobol analysis results, 10,000 different numerical analyses were performed. The variability range explored for the variables of interest, intended as uniform distribution, is given in Table 7.

In general, the Sobol sensitivity study comes to the same conclusions as the generic sensitivity study, confirming the significance of the choice of variables; when different values at different moments of a time history are obtained for different input parameters in the Sobol analysis, it means that these parameters have a different effect on the model output. It appears that the level of interaction of each variable (the difference between the total index and the first order index) does not stay constant during the physical evolution of the phenomenon (Table 8).

Table 7 Intervals of evaluation of the hygro-mechanical properties for the Sobol analysiswhat w

	D_o [$m^2 \cdot s^{-1}$]	Ec1 [$m \cdot s^{-1}$]	Ep [MPa]	X	Y
Lower bound	5.0 10^{-10}	5.0 10^{-09}	1000	0.5	0.5
Upper bound	5.0 10^{-09}	5.0 10^{-07}	5000	1.5	1.5

Hygro-mechanical identification

Figure 7 shows, in the case of waterproofed WPP 5, the results of the optimisation process carried out on the two individual measurements lines of the DK (upper and lower), the quantity actually measured by the system.

In Figs. 8, 9 , 10 and Table 9 the results of the case-by-case optimisation are shown in terms of the angle of curvature; for the sign convention of the angle of curvature, we use the convention described in [28]. Each graph gives the raw data of cupping angle (experimental raw), the data obtained from the smoothing and interpolation process (experimental smoothed) and the numerical results (numerical) at the end of the optimisation, accompanied by the R^2 value calculated between the experimental smoothed and numerical.

Discussion

The sensitivity analysis provides interesting insights, firstly, in term of the level of complexity of the phenomenon. Any variation in the input variables leads to a consistent variation in the trend of the curves, imposing completely different slopes on the time history. This, confirming [16], shows the great variability of the physical

Table 8 Sobol's sensitivity analysis for the cupping angle value obtained after 3, 6 and 9 days after the humidity step change (Do -Diffusion coeff., Ec1Back side emissivity, Ep Rigidity of paint layers, X and Y corrective coeff.s.)

Index	3 days		6 days		9 days	
	First order index	Total index	First order index	Total index	First order index	Total index
D_o	0.25	0.27	0.28	0.37	0.39	0.45
Ec1	0.2	0.2	0.31	0.42	0.22	0.24
Ep	0.43	0.44	0.12	0.14	0.12	0.13
X	0.01	0.02	0.12	0.27	0.2	0.25
Y	0.11	0.12	0.17	0.19	0.07	0.09

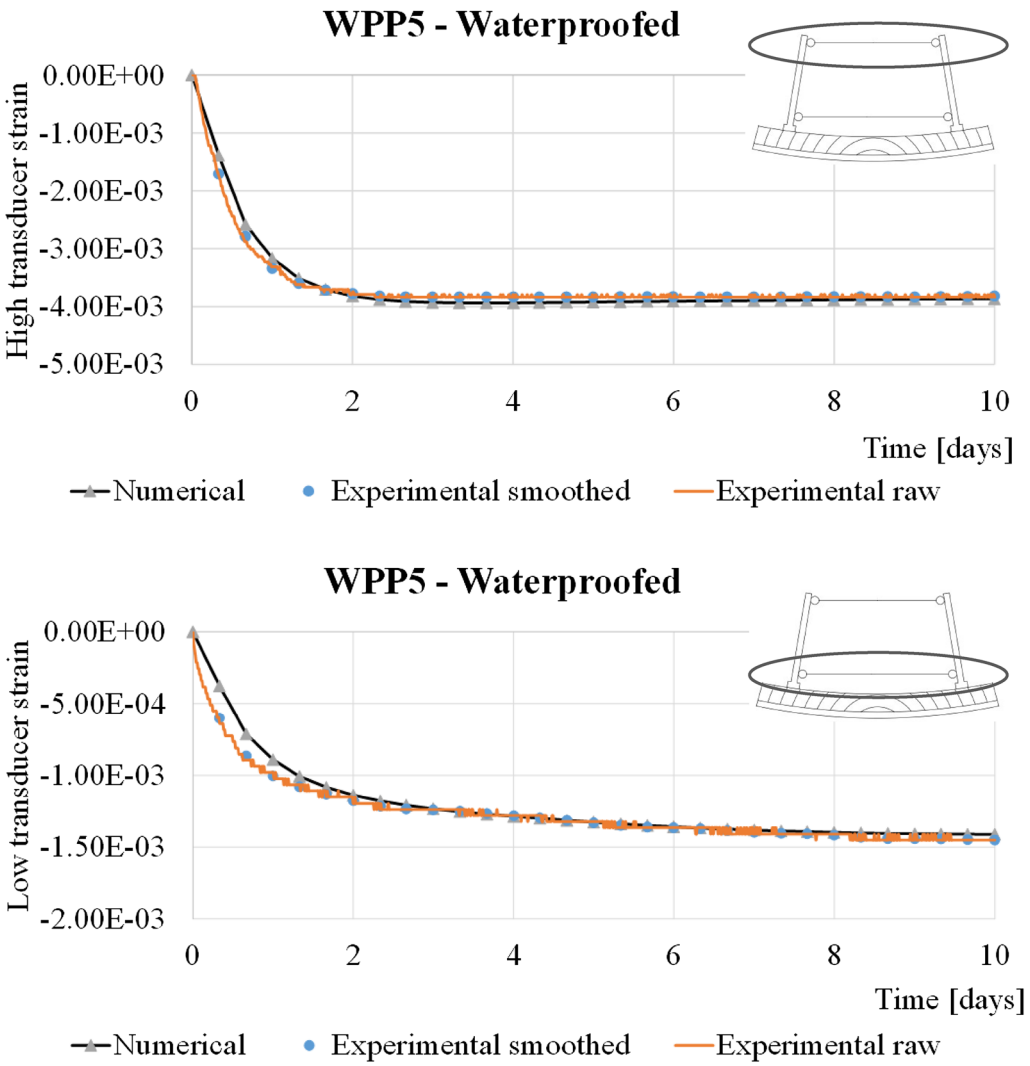

Fig. 7 The results of the optimisation of each DK measurement line (strain [m/m]) from which the cupping angle is derived. High line at the top and low line at the bottom

problem under consideration; even a single incorrectly calibrated variable can lead to results far from reality. Sobol's analysis is a powerful tool for investigating the sensitivity of a model's output to its input parameters. In this context, the analysis reveals a high level of complexity in the deformation tendency of the board, as measured by the cupping angle, and how it varies over time. The analysis also provides a hierarchy of the influence of the input variables on the deformation tendency of the board, highlighting the most significant factors at different time points. The analysis shows that the indices for individual input variables vary greatly over time, while remaining significant, indicating the complex and dynamic nature of the problem. This suggests that the deformation tendency of the board is affected by a combination of factors, with their relative importance changing over time. Additionally, the analysis reveals that there is generally a significant deviation between the first-order index and the total index in the 6-day and 9-day analyses, while they coincide to a first approximation in the 3-day analysis. The first-order index measures the sensitivity of the model output to individual input parameters, while the total index takes into account the interactions between input parameters of different orders. The deviation between the two indices in the 6-day and 9-day analyses indicates the presence of higher-order interactions between input parameters, which have a significant impact on the deformation tendency of the board. This further highlights the complex and dynamic nature of the problem, and the importance of considering higher-order

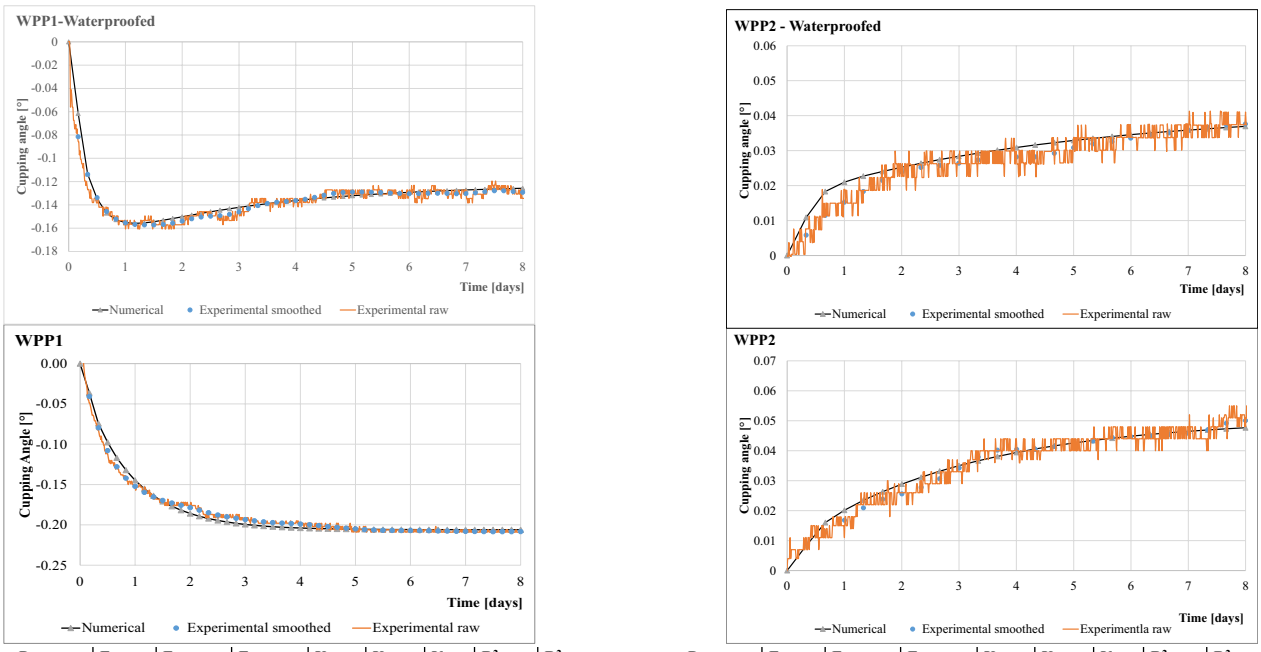

D_0 [$m^2 \cdot s^{-1}$]	E_p [MPa]	E_c [$m \cdot s^{-1}$]	E_{c1} [$m \cdot s^{-1}$]	X wp	X	Y	R^2 wp	R^2
$4\ 10^{-10}$	1506	$7.5\ 10^{-8}$	$9\ 10^{-8}$	0.47	0.62	0.82	0.95	0.99

D_0 [$m^2 \cdot s^{-1}$]	E_p [MPa]	E_c [$m \cdot s^{-1}$]	E_{c1} [$m \cdot s^{-1}$]	X wp	X	Y	R^2 wp	R^2
$4.5\ 10^{-9}$	2613	$4\ 10^{-8}$	$1.1\ 10^{-7}$	0.3	0.3	0.57	0.99	0.99

Fig. 8 Results of the optimisation for WPP1 (on the left) and WPP2 (on the right). For each WPP, on top the optimisation when waterproofed and below when no-waterproofed. The table resuming the hygro-mechanical characteristics and correlation coefficients (D_o -Diffusion coeff., E_{c1} Back side emissivity, E_p Rigidity of paint layers, X and Y corrective coeff.s.; wp means waterproofed, if wp is not present the results are for no-waterproofed WPPs)

interactions in the sensitivity analysis. Overall, Sobol's analysis provides valuable insights into the sensitivity of the model's output to its input parameters, revealing the complex and dynamic nature of the deformation tendency of the board and the changing importance of input parameters over time. The analysis highlights the importance of considering higher-order interactions in the sensitivity analysis, which can help improve the accuracy and reliability of the model. This difference has the significance of denoting an interaction of the input variables, i.e. the extent to which the distribution of one variable can be influenced by the variation in the distribution of another variable. In simplified terms, we can say that two inputs have an interaction if their combined effect on the output is greater than the sum of their effects considered separately. This is equivalent to saying that variations in the ambient RH cause a variation in the MC of the hygroscopic materials of which the work is composed, and as a result it manifests a deformation behaviour that is the result of the interaction between the anatomy of the boards and the stiffness and diffusivity of the preparation layers and the colour. The fact that the interaction of variables with each other makes them more significant is therefore a fact that should not be underestimated and shows us that it is necessary to evaluate them precisely in their interaction, i.e. in the actual physical situation. It also shows us a strong system effect, which, coupled with the consideration that in this context small variations in the input variables lead to large variations in the kinetic configuration of the system, is typical of systems with a high level of complexity.

Sensitivity analysis also can be evaluated in how uncertainties in the input variables are carried into the model's response; in this view we can easily observe how the use of material properties not calibrated to the work, but, for example, extracted from literature values or simulacra, lead to enormously valuable variations on the solution, confirming the results of [16].

Regarding the results of the optimization process, it can be observed that the iterative process leads us to numerical results that tend to agree with the experimental data, with the majority of the results presenting a determination coefficient (R^2) of 0.99. The most important indications from this are that the chosen variables and modelling assumptions are essentially a sufficient description of the physical system, and that numerical models can be successfully calibrated.

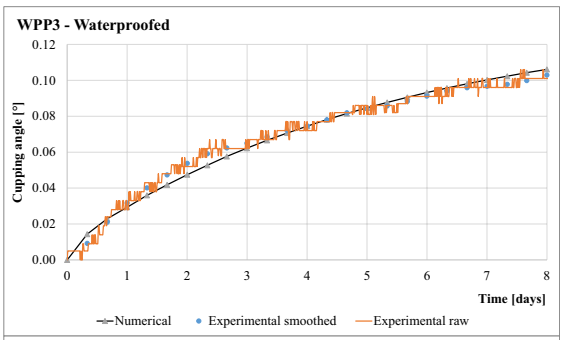

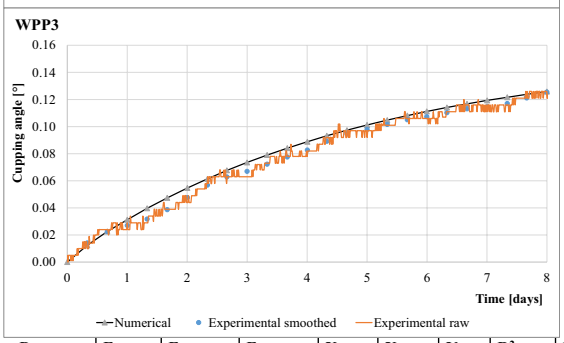

D_0	E_p	E_c	E_{c1}	X	X	Y	R^2	R^2
$[m^2 \cdot s^{-1}]$	[MPa]	$[m \cdot s^{-1}]$	$[m \cdot s^{-1}]$	wp			wp	
$1.6\ 10^{-8}$	11467	$4.3\ 10^{-8}$	$5\ 10^{-8}$	0.51	0.80	0.93	0.99	0.99

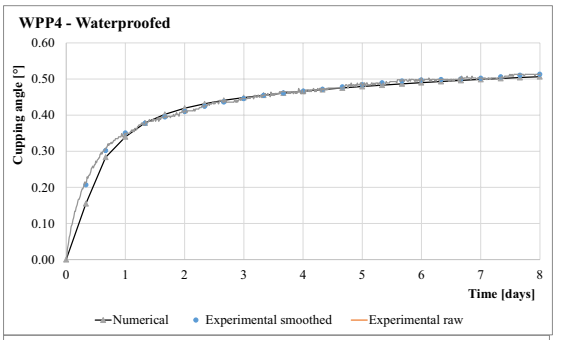

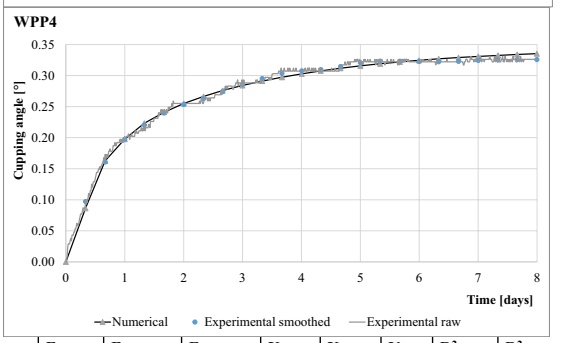

D_0	E_p	E_c	E_{c1}	X	X	Y	R^2	R^2
$[m^2 \cdot s^{-1}]$	[MPa]	$[m \cdot s^{-1}]$	$[m \cdot s^{-1}]$	wp			wp	
$6\ 10^{-10}$	10500	$3\ 10^{-8}$	$1.8\ 10^{-7}$	2.2	2.05	1.5	0.99	0.99

Fig. 9 Results of the optimisation for WPP3 (on the left) and WPP4 (on the right). For each WPP, on top the optimisation when waterproofed and below when no-waterproofed. The table resuming the hygro-mechanical characteristics and correlation coefficients (Do -Diffusion coeff., Ec1Back side emissivity, Ep Rigidity of paint layers, X and Y corrective coeff.s.; wp means waterproofed, if wp is not present the results are for no-waterproofed WPPs)

The logical consequence is that the input parameters of the model can be considered as representative of those that can be associated with the real phenomenon. In any case these are averaged parameters, subject to constitutive and modelling assumptions, underlying a stringent assumption of material homogeneity, etc., and are therefore themselves subject to margins of uncertainty, but nevertheless they allow a model built on them to behave like the real object.

The numerical values obtained from the optimization process (tables in Figs. 8, 9 and 10), show a large dispersion in the numerical values of each parameter between the different WPPs studied. In particular the values obtained for the stiffness of the paint layers are very variable, in the range identified by [9], and allow us to identify in WPP1, WPP5, WPP6 as panels with paint layers of low stiffness, which doesn't prevent their flying-wood behaviour in the sealed state, confirming the qualitative analyses of [16].

WPP3 requires a special attention as the support wood is found to have a high transverse diffusivity. Observing the artwork, the restorers pointed out the presence of a protective layer of impregnating waterproofing beeswax on the back. One hypothesis to explain this early restoration choice, made in the distant past and undocumented, is that the work was probably extremely reactive and the restorers wanted to balance the emissivity of the back against the front by using of a waterproofing product. The result is in fact a board with a very high diffusivity in general, with both sides having the same emissivity, which then moves with almost symmetrical internal gradients, due to the cylindrical anisotropy characteristics of the shrinkage/swelling and the stiffness relationship between the wood and the preparation.

The optimisation process failed to find consistent parameters to fit the first part of uncoated WPP5 test. It is difficult to understand the cause of this localised deviation, given the excellent agreement of the waterproofed test. In fact, it should be noted that only the emissivity of the painted surface and the hygroscopic strain multiplier vary between the first and the second test; if the multiplier essentially leads to a vertical shift of the curve, there is no emissivity value that leads to the match. In our opinion, the cause of this could be a material inhomogeneity just below the interface between the preparation layers and the wood,

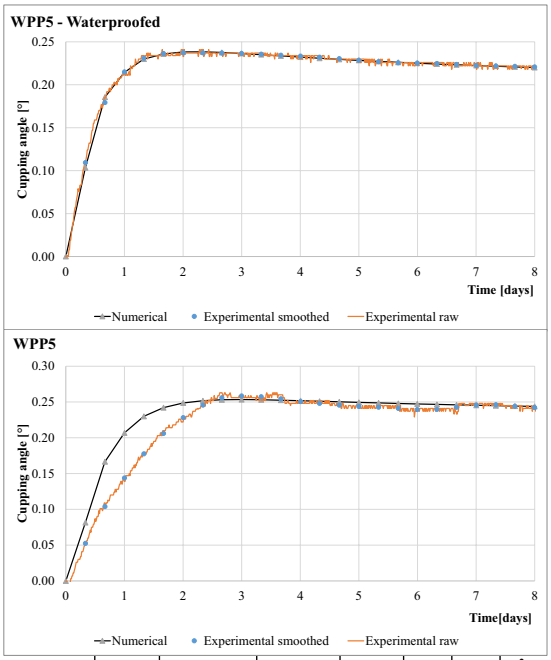

D_0 [$m^2 \cdot s^{-1}$]	E_p [MPa]	E_c [$m \cdot s^{-1}$]	E_{c1} [$mm \cdot s^{-1}$]	X wp	X	Y	R^2 wp	R^2
1.1 10^{-9}	1952	1 10^{-10}	2.6 10^{-7}	1.27	1.29	0.55	0.99	0.89

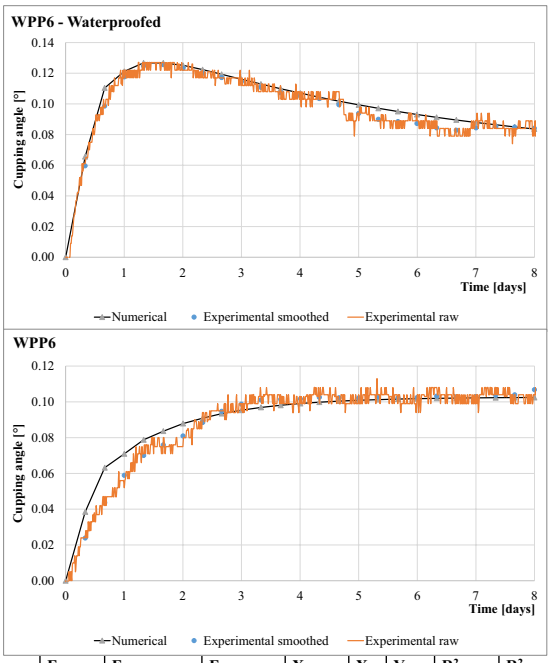

D_0 [$m^2 \cdot s^{-1}$]	E_p [MPa]	E_c [$m \cdot s^{-1}$]	E_{c1} [$m \cdot s^{-1}$]	X wp	X	Y	R^2 wp	R^2
.9 10^{-10}	563	3 10^{-7}	5 10^{-7}	0.67	1.2	0.45	0.97	0.98

Fig. 10 Results of the optimisation for WPP5 (on the left) and WPP6 (on the right). For each WPP, on top the optimisation when waterproofed and below when no-waterproofed. The table resuming the hygro-mechanical characteristics and correlation coefficients (Do -Diffusion coeff., Ec1Back side emissivity, Ep Rigidity of paint layers, X and Y corrective coeff.s.; wp means waterproofed, if wp is not present the results are for no-waterproofed WPPs)

Table 9 Summary of the calculated hygro-mechanical values for the studied WPPs (Do -Diffusion coeff., Ec1Back side emissivity, Ep Rigidity of paint layers, X and Y corrective coeff.s.; wp means waterproofed and no wp means no-waterproofed

	D_0 [$m^2 \cdot s^{-1}$]	E_p [MPa]	E_c [$m \cdot s^{-1}$]	E_{c1} [$m \cdot s^{-1}$]	X wp	X no wp	Y
WPP1	4.0 10^{-10}	1506	7.5 10^{-08}	9.0 10^{-08}	0.47	0.62	0.82
WPP2	4.5 10^{-09}	2613	4.0 10^{-08}	1.1 10^{-07}	0.3	0.3	0.57
WPP3	1.6 10^{-08}	11467	4.3 10^{-08}	5.0 10^{-08}	0.51	0.8	0.93
WPP4	6.0 10^{-10}	10500	3.0 10^{-08}	1.8 10^{-07}	2.2	2.05	1.5
WPP5	1.1 10^{-09}	1952	1.0 10^{-10}	2.6 10^{-07}	1.27	1.29	0.55
WPP6	9.0 10^{-10}	563	3.0 10^{-07}	5.0 10^{-07}	0.67	1.2	0.45

or an experimental problem whose cause we could not understand.

In general, the numerical results are qualitatively slightly different from the experimental evidence in the very early stages of the transient. As shown by the local sensitivity study, at this early stage the differences that the different variables have on the initial part of the ramp are not discernible. Apart from the fact that this phase was also the most critical for the humidity generator, which needs time to stabilise the humidity in the chamber after the change, it seems to us that the main cause of this discordance is due to a local inhomogeneity in the first layers of the wood back. In these first transient moments, the internal moisture gradient of the wood only affects the first few millimetres, which act as a deformation motor for the rest of the section, which tends to maintain its size, still at the previous moisture content. The most likely causes are: ageing, damage, general inhomogeneity such as insect

infestation. In any case, this is an interesting topic for future research.

Conclusions

Based on experiments on original paintings subjected to controlled thermo-hygrometric variations, a simplified physical model was developed. After methods of uncertainty analysis were applied to analyse the complexity and sensitivity of the problem, the model was calibrated on experimental tests, leading to hygro-mechanical characterisation of each studied panel.

Based on the results presented, the study demonstrated the possibility of non-invasively characterising a WPP in its complexity through direct observation of its behaviour. The parameterisation of the variables obtained by this approach then makes it possible to model its behaviour and virtually explore hypothetical conservation scenarios. While taking into account the classical limitations associated with inverse identification methods, such as the strong dependence on the physical model chosen and the enormous computational burden, and in the case of emissivity the active stirring of air, the characteristics identified—an approximation to the real ones, assuming that they can be unambiguously identified in the real object—allow the construction of numerical models whose behaviour is highly congruent with the real one. There is no guarantee that in general experimentation framework, different from the one described here, inverse analysis would be successful in the case of panel paintings. However, in the specific context described in this paper it has been shown to be effective and promising if combined with the use of appropriate modelling and experimental testing. A significant amount of effort was invested in determining the minimum number of variables required to ensure the effectiveness of the process while maintaining its full physical relevance.

The research has also shown that, in order to understand and model the hygromechanical phenomena that govern the deformation tendencies of paintings on panels, it is necessary to consider a strategy of direct analysis on the object, which, at the current state of knowledge, seems to be the only way to avoid obtaining results that have nothing to do with reality. The strategy that this study proposes, beyond the characterisation tools and techniques that can be applied or implemented, is that of "learning from objects". We therefore start by asking the object what its deformation tendencies are, through experimental investigations. In this context, numerical analysis becomes a method to be developed in parallel with experiments and which helps to increase the level of knowledge and extract as much information as possible.

Appendix 1

Description of the implementation of the elastic orthotropic behaviour of the wooden panel in MFront.

This appendix describes how the of the elastic orthotropic behaviour of the wooden panel has been implemented using the open source-code generator MFront co-developed under strict assurance quality constraints by CEA, EDF and Framatome in the context of a numerical plateform dedicated to the simulation of the nuclear fuel elements named PLEIADES. MFront is distributed as part of the Salomé-Méca platform and is tightly integrated with code_aster.

Notations used.

Symbol	Description
$\underline{\underline{\varepsilon}}$	Total strain in the reference system
$\underline{\underline{\varepsilon}}^{\star}$	Total strain in the material frame
$\underline{\underline{\varepsilon}}_{-hyg}$	Hygromechanical strain in the reference system
$\underline{\underline{\varepsilon}}^{\star}_{-hyg}$	Hygromechanical strain in the material frame
$\underline{\underline{\mathbf{C}}}$	Stiffness tensor in the reference system
$\underline{\underline{\mathbf{C}}}^{\star}$	Stiffness tensor in the material frame

In the material frame, the orthotropic elastic behaviour amounts to the following relationship between the total strain $\underline{\underline{\varepsilon}}^{\star}$ and the stress $\underline{\underline{\sigma}}^{\star}$:

$$\underline{\underline{\sigma}}^{\star} = \underline{\underline{\mathbf{C}}}^{\star} : \left(\underline{\underline{\varepsilon}}^{\star} - \underline{\underline{\varepsilon}}^{\star}_{-hyg}\right) \tag{14}$$

where $\underline{\underline{\mathbf{C}}}^{\star}$ denotes the stiffness tensor in the material frame.

Let $\underline{\underline{\mathbf{R}}}$ the fourth order tensor such that:

$$\begin{cases} \underline{\underline{\varepsilon}} = \underline{\underline{\mathbf{R}}} : \underline{\underline{\varepsilon}}^{\star} \\ \underline{\underline{\sigma}} = \underline{\underline{\mathbf{R}}} : \underline{\underline{\sigma}}^{\star} \end{cases} \tag{15}$$

Then, the Constitutive Eq. 17 can be rewritten as follows:

$$\underline{\underline{\sigma}} = \left(\underline{\underline{\mathbf{R}}}\right)^{-1} \cdot \underline{\underline{\mathbf{C}}}^{\star} \cdot \underline{\underline{\mathbf{R}}} : \left(\underline{\underline{\varepsilon}} - \underline{\underline{\varepsilon}}_{-hyg}\right) \tag{16}$$

or, equivalently:

$$\underline{\underline{\sigma}} = \underline{\underline{\underline{\underline{\mathbf{C}}}}} : \left(\underline{\underline{\varepsilon}} - \underline{\underline{\varepsilon}}_{hyg} \right) \tag{17}$$

With

$$\underline{\underline{\underline{\underline{\mathbf{C}}}}} = \left(\underline{\underline{\mathbf{R}}} \right)^{-1} \cdot \underline{\underline{\underline{\underline{\mathbf{C}}^{\star}}}} \cdot \underline{\underline{\mathbf{R}}} \tag{18}$$

MFront provides the mandatory functions to build $\underline{\underline{\varepsilon}}_{hyg}$ and from the two rotation matrices corresponding to composition of the rotation in the cylindrical frame and to material frame.

Appendix 2

In its most widely used configuration, the DK basically consists of (a) two metal columns secured in a minimally invasive manner on the back face of a painted panel in such a way that they stand perpendicular to the wood surface, and (b) two displacement transducers (that constitute the Upper and Lower Measurement Line), whose opposite ends are hinged on the two columns, measuring the distance between them at fixed distances from the wood surface (Fig. 9). The outputs from the transducers are sampled at chosen time intervals, and the resulting data are stored in the memory of a data-logger for further analysis. The line connecting the points in which the axes of the two columns intersect the back face of the panel, should be as perpendicular as possible to the direction of the wood grain. As the panel deforms (for any reason, including environmental variations and applied bending moments) the two columns move and rotate relative to each other, and the centres of the spherical hinges connecting each transducer to the columns move closer together or further apart. The more the deformation of the panel approximates pure cupping without twisting and the rings in the cross-section under the measurement lines are not inclined with respect to the longitudinal direction of the board, the more the two columns remain in the same plane. So that the variations in distance measured by the transducers allow the exact reconstruction, instant by instant, of the cupping angle (i.e. the angle formed by the axes of the columns), based on the geometry of the panel-transducers-columns system (Fig. 9).

Acknowledgements
This research received specific grant from Tuscan Region, Italy (PREMUDE Project—POR-FSE 2014–2020. Modelli innovativi per la conservazione PREventiva in ambienti MUseali e DEpositi temporanei post-emergenza).

Author contributions
LR conceived and discussed the theoretical approach, the methods implemented and the numerical procedures applied, did every step of the modelling, developed the behaviour law of wood, analysed the models and extracted the conclusions, developed the experimental investigations, wrote and revised the paper. PM developed the experimental investigations, discussed the results and revised the paper. TH developed the behaviour law of wood. CM developed the experimental investigations, revised the paper. LU developed the experimental investigations, revised the paper. LR, SR, AS and CC chose and provide the six historical panel paintings, participated in designing the tests and revised the paper. JG discussed the methods implemented and the numerical procedures applied, reviewed and discussed the numerical results, revised the paper. MF conceived and discussed the theoretical approach, discussed the methods implemented and the numerical procedures applied, reviewed and discussed the results, wrote and revised the paper, coordinated the project. All authors read and approved the final manuscript.

Availability of data and materials
Data are available from the corresponding author [P.M.] upon reasonable request and with permission of the Superintendence that owns the panel paintings.

Declarations

Competing interests
The authors declare that they have no known competing financial interests or personal relationships that could have appeared to influence the work reported in this paper.

Received: 26 January 2023 Accepted: 17 May 2023
Published online: 14 June 2023

References

1. C. Cennini, Il libro dell'arte, Neri Pozza. Frezzato F., 2009. The art book, in Italian,
2. L. Uzielli. Historical overview of panel-making techniques in central Italy, in proceedings of a symposium at the J. Paul Getty Museum 24–28 April 1995. The Getty Conservation Institute, US 1998; 110–135.
3. J. Wadum. Historical overview of panel-making techniques in northern countries, in proceedings of a symposium at the J. Paul Getty Museum 24–28 April 1995. The Getty Conservation Institute, US 1998; 149–177.
4. J Gril, D Jullien, D Hunt. Compression set and cupping of painted wooden panels, in analysis and characterisation of wooden cultural heritage by scientific engineering methods, Halle (Saale), Germany, April 2016. https://hal.archives-ouvertes.fr/hal-01452161. Accessed 12 June 2023.
5. M Mecklenburg, C Tumosa, D Erhardt. Structural response of painted wood surfaces to changes in ambient relative humidity, in Painted Wood: History and Conservation. The Getty Conservation Institute, US 1998; 464–483.
6. Allegretti O, De Vincenzi M, Uzielli L, Dionisi-Vici P. Long-term hygro-mechanical monitoring of Wooden Objects of Art (WOA): a tool for preventive conservation. J Cult Herit. 2013;14(3):e161–4. https://doi.org/10.1016/j.culher.2012.10.022.
7. Dupre J-C, Jullien D, Uzielli L, Hesser F, Riparbelli L, Gauvin C, et al. Experimental study of the hygromechanical behaviour of a historic painting on wooden panel: devices and measurement techniques. J Cult Herit. 2020;46:165–75. https://doi.org/10.1016/j.culher.2020.09.003.
8. J Colmars, B Marcon, E Maurin, R Remond, F Morestin, P Mazzanti, J Gril. Hygromechanical response of a panel painting in a church, monitoring and computer modeling, in International conference on wooden cultural heritage, Evaluation of deterioration and management of change, Hamburg, Germany, 2009., p. 9. https://hal.archives-ouvertes.fr/hal-00795990. Accessed 12 June 2023.
9. C. Gauvin. Etude expérimentale et numérique du comportement hygro-mécanique d'un panneau de bois : application à la conservation des tableaux peints sur bois du patrimoine, PhD Thesis, LMGC - Laboratoire de Mécanique et Génie Civil, Université de Montpellier 2, 2015. Experimental study and numerical modelling of the hygromechanical behaviour of wood applied to the conservation of panel paintings, in French.

10. Mazzanti P, Togni M, Uzielli L. Drying shrinkage and mechanical properties of Poplar wood (Popolus alba L.) across the grain. J Cult Herit. 2012;13(3):S85–9.
11. Mazzanti P, Colmars J, Gril J, Hunt D, Uzielli L. A hygro-mechanical analysis of poplar wood along the tangential direction by restrained swelling test. Wood Sci Technol. 2014;48:673–87. https://doi.org/10.1007/s00226-014-0633-4.
12. Hunt D, Uzielli L, Mazzanti P. Strains in gesso on painted wood panels during humidity changes and cupping. J Cult Herit. 2017;25:163–9.
13. Allegretti O, Raffaelli F. Barrier effect to water vapour of early European painting materials on wood panels. Stud Conserv. 2008;53(3):187–97. https://doi.org/10.1179/sic.2008.53.3.187.
14. Stöcklein J, Konopka D, Grajcarek G, Tietze O, Oertel S, Schulze A, Kaliske M. Hygro-mechanical short-term behaviour of selected coatings: experiments and material modelling on vapour permeability and mechanical properties. Herit Sci. 2022;10(1):141. https://doi.org/10.1186/s40494-022-00768-5.
15. Janas A, Mecklenburg MF, Fuster-López L, Kozłowski R, Kékicheff P, Favier D, Krarup Andersen C, Scharff M, Bratasz Ł. Shrinkage and mechanical properties of drying oil paints. Herit Sci. 2022;10(1):181. https://doi.org/10.1186/s40494-022-00814-2.
16. Riparbelli L, Mazzanti P, Manfriani C, Uzielli L, Castelli C, Gualdani G, Ricciardi L, Santacesaria A, Rossi S, Fioravanti M. Hygromechanical behaviour of wooden panel paintings: classification of their deformation tendencies based on numerical modelling and experimental results. Herit Sci. 2023. https://doi.org/10.1186/s40494-022-00843-x.
17. J. Froidevaux. Wood and paint layers aging and risk analysis of ancient panel painting, PhD Thesis, Université Montpellier 2, 2012.
18. Dureisseix D, Marcon B. A partitioning strategy for the coupled hygromechanical analysis with application to wood structures of cultural heritage. Int J Numer Methods Eng. 2011;88(3):228–56.
19. Gebhardt C, Konopka D, Börner A, Mäder M, Kaliske M. Hygro-mechanical numerical investigations of a wooden panel painting from "Katharinenaltar" by Lucas Cranach the Elder. J Cult Herit. 2018;29:1–9.
20. Saft S, Kaliske M. Numerical simulation of the ductile failure of mechanically and moisture loaded wooden structures. Comput Struct. 2011;89(23–24):2460–70. https://doi.org/10.1016/j.compstruc.2011.06.004.
21. Rachwał B, Bratasz Ł, Krzemień L, Łukomski M, Kozłowski R. Fatigue damage of the Gesso layer in panel paintings subjected to changing climate conditions. Strain. 2012;48(6):474–81. https://doi.org/10.1111/j.1475-1305.2012.00844.x.
22. Rachwał B, Bratasz Ł, Łukomski M, Kozłowski R. Response of wood supports in panel paintings subjected to changing climate conditions. Strain. 2012;48(5):366–74. https://doi.org/10.1111/j.1475-1305.2011.00832.x.
23. Kupczak A, Jędrychowski M, Strojecki M, Krzemień L, Bratasz Ł, Łukomski M, Kozłowski R. HERIe: a web-based decision-supporting tool for assessing risk of physical damage using various failure criteria. Stud Conserv. 2018;63(1):151–5. https://doi.org/10.1080/00393630.2018.1504447.
24. Dionisi-Vici P, Mazzanti P, Uzielli L. Mechanical response of wooden boards subjected to humidity step variations: climatic chamber measurements and fitted mathematical models. J Cult Herit. 2006;7(1):37–48.
25. Allegretti O, Bontadi J, Dionisi-Vici P. Climate induced deformation of Panel Paintings: experimental observations on interaction between paint layers and thin wooden supports. Int Conf Florence Heri-Tech Future Herit Sci Technol. 2020. https://doi.org/10.1088/1757-899X/949/1/012018.
26. Krzemień L, Łukomski M, Bratasz Ł, Kozłowski R, Mecklenburg MF. Mechanism of craquelure pattern formation on panel paintings. Stud Conserv. 2016;61(6):324–30. https://doi.org/10.1080/00393630.2016.1140428.
27. Marcon B, Goli G, Fioravanti M. Modelling wooden cultural heritage. The need to consider each artefact as unique as illustrated by the Cannone violin. Herit Sci. 2020;8(1):24. https://doi.org/10.1186/s40494-020-00368-1.
28. Uzielli L, Cocchi L, Mazzanti P, Togni M, Julien D, Dionisi-Vici P. The Deformometric Kit: a method and an apparatus for monitoring the deformation of wooden panels. J Cult Herit. 2012;13(3):94–101.
29. P. Dionisi-Vici, I. Bucciardini, M. Fioravanti, L. Uzielli. Monitoring climate and deformation of panel paintings in San Marco (Florence) and other Museums, COST IE0601 international conference on wood science for conservation of cultural heritage, Florence, Italy, 2009; 193–199.
30. P. Dionis-Vici, M. Formosa, J. Schiro, L. Uzielli. Local deformation reactivity of panel paintings in an environment with random microclimate variations: the Maltese Maestro Alberto's Nativity case-study, COST IE0601 international conference on wood science for conservation of cultural heritage, Braga (PT), 2008.
31. L. Cocchi, G. Goli, P. Mazzanti, B. Marcon, L. Uzielli. The Lapidazione di Santo Stefano by Giorgio Vasari: the study of the wooden support's deformations as a contribution to restoration and future conservation, in Proceedings of ESRARC 2014 6th European Symposium on Religious Art, Restoration & Conservation, Florence (Italy), 2014.
32. Cocchi L, Marcon B, Goli G, Mazzanti P, Castelli C, Santacesaria A, Uzielli L. Verifying the operation of an elastic crossbar system applied to a panel painting: the deposition from the Cross by an anonymous artist from Abruzzo, sixteenth century. Stud Conserv. 2017;62(3):150–61. https://doi.org/10.1080/00393630.2015.1137426.
33. Bremaud I, Gril J. Transient destabilisation in anisotropic vibrational properties of wood when changing humidity. Holzforschung. 2021;75(4):328–44. https://doi.org/10.1515/hf-2020-0029.
34. EDF - Électricité De France, Finite element Code_Aster: Analyse des Structures et Thermo-mécanique pour des Etudes et des Recherches. 2022.
35. Helfer T, Michel B, Proix J-M, Salvo M, Sercombe J, Casella M. Introducing the open-source mfront code generator: application to mechanical behaviours and material knowledge management within the PLEIADES fuel element modelling platform. Comput Math Appl. 2015;70(5):994–1023. https://doi.org/10.1016/j.camwa.2015.06.027.
36. M. Varnier, L. Ulmet, F. Dubois, N. Sauvat. Characterization and modeling of wood species sorption isotherms for use in civil engineering structures monitoring, In Review, preprint, 2022. doi: https://doi.org/10.21203/rs.3.rs-2113454/v1.
37. Merakeb S, Dubois F, Petit C. Modeling of the sorption hysteresis for wood. Wood Sci Technol. 2009;43(7):575–89. https://doi.org/10.1007/s00226-009-0249-2.
38. HL Frandsen. Selected constitutive models for simulating the hygromechanical response of wood, Ph.D. thesis, Aalborg University, 2007.
39. Assimi H, Jamali A. A hybrid algorithm coupling genetic programming and Nelder-Mead for topology and size optimization of trusses with static and dynamic constraints. Expert Syst Appl. 2018;95:127–41. https://doi.org/10.1016/j.eswa.2017.11.035.
40. NE Mastorakis. On the solution of ill-conditioned systems of linear and non-linear equations via genetic algorithms (GAs) and Nelder-Mead simplex search, in proceedings of the 6th WSEAS international conference on evolutionary computing, Stevens Point, Wisconsin, USA, 2005; pp. 29–35.
41. NE Mastorakis. Solving non-linear equations via genetic algorithms, Proceedings of the 6th WSEAS Int. Conf. on EVOLUTIONARY COMPUTING, Lisbon, Portugal, June 16–18, 2005. https://citeseerx.ist.psu.edu/document?repid=rep1&type=pdf&doi=cc57ed0b649647f04da29af1e57fc6d2b435644f, last checked December 2022.
42. M Baudin, A Dutfoy, A Geay, A-L Popelin, A Ladier, J Schueller, T Yalamas. The graphical user interface of OpenTURNS, a UQ software in simulation, in proceedings of the 2nd international conference on uncertainty quantification in computational sciences and engineering (UNCECOMP 2017), Rhodes Island, Greece, 2017, pp. 238–257. doi: https://doi.org/10.7712/120217.5366.17143.
43. Baudin M, Dutfoy A, Iooss B, Popelin A-L. OpenTURNS: an industrial software for uncertainty quantification in simulation. In: Ghanem R, Higdon D, Owhadi H, editors. Handbook of uncertainty quantification. Cham: Springer International; 2017. p. 2001–38. https://doi.org/10.1007/978-3-319-12385-1_64.
44. Z Kala, J Kala, TE Simos, G Psihoyios, Ch Tsitouras, Z Anastassi. Sensitivity analysis of stability problems of steel structures using shell finite elements and nonlinear computation methods, NUMERICAL ANALYSIS AND APPLIED MATHEMATICS ICNAAM 2011: international conference on numerical analysis and applied mathematics, Halkidiki, (Greece), 2011; 1865–1868. https://doi.org/10.1063/1.3636974.

45. Cartailler T, Guaus A, Janon A, Monod H, Prieur C, Saint-Geours N. Sensitivity analysis and uncertainty quantification for environmental models. ESAIM Proc. 2014;44:300–21. https://doi.org/10.1051/proc/201444019.
46. Du W, Li S, Luo Y. Implementation of Sobol's sensitivity analysis to cyclic plasticity model with parameter uncertainty. Int J Fatigue. 2021;155:106578. https://doi.org/10.1016/j.ijfatigue.2021.106578. Accessed 12 June 2023.
47. Zhang X, Trame M, Lesko L, Schmidt S. Sobol sensitivity analysis: a tool to guide the development and evaluation of systems pharmacology models. CPT Pharmacomet Syst Pharmacol. 2015;4(2):69–79. https://doi.org/10.1002/psp4.6.

Publisher's Note